New Evidence Derived from the Discrimination of Henry and Langmuir Modes Parameters in Glassy Polymeric Film Revealed by the Freeze-Purged-Desorption Method

Junya Togawa, Masayoshi Kobayashi

Department of Chemical System Engineering, Kitami Institute of Technology, 165 Koen-cho, Kitami, Hokkaido 090-8507, Japan

Received 25 August 2003; accepted 30 December 2003
DOI 10.1002/app.20527
Published online in Wiley InterScience (www.interscience.wiley.com).

ABSTRACT: The Freeze-Purged-Desorption (FPD) method was developed for the experimental measurement of gas permeability coefficients as a new technique using a desorption curve of gas immobilized in polymeric films. The FPD method was effectively used to evaluate four gas permeation parameters (C_D, C_H, D_D, and D_H) of glassy polymeric films (polycarbonate and polystyrene) by using CO_2. The modes of the CO_2 gas desorption response curve (D-curve) obtained were sensitively characterized by the proportion of sorption in the Henry and Langmuir modes in the polymeric films accompanied by their own gas diffusivity. A graphical analysis of the D-curve of CO_2 reasonably proposed a linear relation between the desorption rate and the sorption amount of CO_2, which was strongly influenced by the kind of sorption gas, film, temperature, and other factors. The desorption rate of sorbed CO_2 gas for the PC and PS films gave a characteristic straight line with an inflection point indicating a shift in the gas-diffusion mechanism from the complex type of the Henry and the Langmuir modes to the Langmuir mode. The characteristic D-curves obtained were graphically analyzed, and they clearly discriminated the Henry mode part and the Langmuir mode part. This discrimination process quantitatively and individually evaluated C_D, C_H, D_D, and D_H. By using the four parameters evaluated, a mathematical model to describe the D-curve was proposed, and it consistently explained the experimental D-curves. © 2004 Wiley Periodicals, Inc. J Appl Polym Sci 93: 934–941, 2004

Key words: polystyrene; polycarbonate; gas permeation; diffusion; membranes

INTRODUCTION

Quantitative evaluations of gas diffusivity and solubility give important information to design the requested gas separation films. As is well known, gas permeation behaviors for rubbery and glassy polymeric films are characterized by different permeation mechanisms. For rubbery polymeric films, gas permeation was evaluated by the solution-diffusion model, and the gas diffusivity was calculated from the time lag, the initial slope, and the half-steady methods using the gas permeation curve or gas sorption curve that was derived from an approximate solution of Fick's second law of diffusion.[1,2] For glassy polymeric films, it was thought that gas sorption occurred by the dual-sorption mechanism in which Henry dissolution and Langmuir adsorption proceed in parallel at an equilibrium state of gas sorption.[3] To individually evaluate the gas permeation parameters in glassy polymer, Paul and Koros proposed the partial-immobilization model[4] based on dual-mode mobility. This model was dominated by four parameters: the concentration of the Henry dissolution component (C_D), the concentration of the Langmuir adsorption component (C_H), the diffusivity of the Henry mode (D_D), and the diffusivity of the Langmuir mode (D_H). To evaluate the four parameters, it was necessary to gather much experimental data for the amount of sorbed gas and the gas permeability through a glassy polymeric film under a wide range of desired gas pressures.

By using the additional assistance of the evaluation of dual-mode sorption parameters evaluated by both the extrapolation and the linearization of gas-sorption isotherms, the graphical analysis of a curve of permeability as a function of gas partial pressure is required. Although many researchers have focused on the evaluations of dual-sorption parameters,[5–12] few works evaluating the parameters using the partial-immobilization model have been reported.[13–16] As is well known, the gas diffusivity and sorption amount in film evaluated from these conventional procedures sometimes contain serious errors because of the approximation and extrapolation of the data obtained.

To solve this difficulty, in our previous studies,[17,18] the Freeze-Purged-Desorption (FPD) method was de-

Correspondence to: M. Kobayashi (koba@betta.chem.kitami-it.ac.jp).

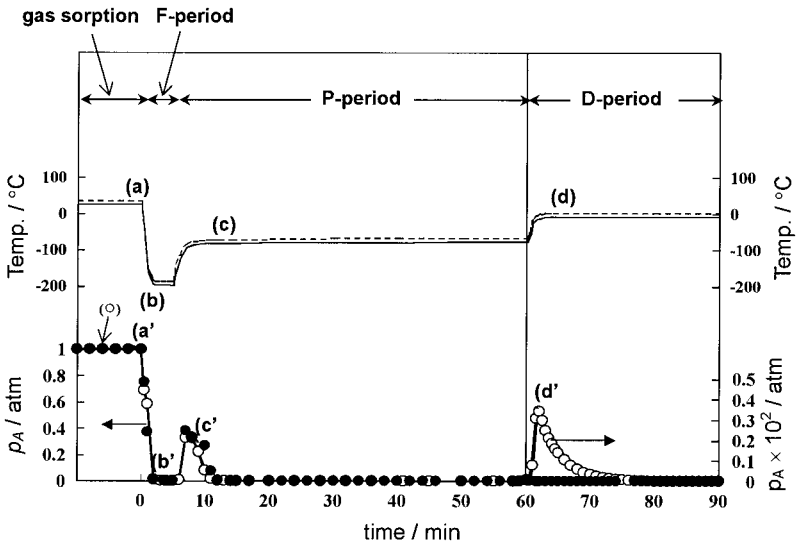

Figure 1 Typical example of temperature and gas desorption response curves for the FPD method. Open circle is for the film-packed cell and closed circle is for the blank cell.

veloped for the simultaneous evaluations of gas solubility and diffusivity in the low-density polyethylene (LDPE) and high-density polyethylene (HDPE) films as rubbery polymers using the graphical analysis of the desorption response curve (D-curve) of sorbed gas observed in a temperature jump-up operation. The validity of the FPD method was reconfirmed by the evaluations of diffusivity and solubility of CO_2 in the two films.[18] The objectives of the current study are, using the FPD method, (1) to discriminate the Henry and Langmuir modes of the D-curve obtained for glassy polymer films; (2) to quantitatively evaluate C_D, C_H, $D_{D,}$ and D_H by a graphical analysis of D-curves; and (3) to compare the four parameters evaluated with reference values.

FPD METHOD

Figure 1 illustrates a schematic explanation for the temperature and gas-desorption response curves obtained by the FPD method. The FPD method consists of three operational periods (freeze, purge, and desorption), each of which is, respectively, characterized by three consecutive stepwise changes in temperature-indicating curves (b), (c), and (d). The freeze period (F-period) is for the fixation of sorbed gas in film at −196°C, by using a liquid nitrogen bath, and the purge period (P-period) is for the removal of residual gas in a gas-sorption cell, except the sorbed gas in the film, by using a helium gas stream at the boiling point of sorbed gas. The desorption period (D-period) is for the desorption of sorbed gas from the film at a specified temperature, which is sufficiently higher than the boiling point of the sorbed gas. The amount of gas sorbed in the film is evaluated from the graphical integration of the D-period curve (D-curve). The gas diffusivity in the film is easily calculated from a graphical analysis of the D-curve obtained.

When the film used is sufficiently thin, the amount of CO_2 desorbed along the thickness is negligibly small, and the rate of CO_2 desorption from the lateral surface is proportional to the sorbed amount in the film, similar to the desorption behavior of adsorbed species on the surface. Accepting this consideration, one can presume the diffusion rate of CO_2 in the film to be equal to the desorption rate. For the evaluation of gas diffusivity in the film, consequently, one can effectively use the relation between the gas desorption rate (dN_A/dt) from the film and the residual amount of gas sorbed in the film (ΔC_A) at any elapsed time by

$$\frac{dN_A}{dt} = \frac{2AD}{L}\Delta C_A \tag{1}$$

where N_A is cm^3 [standard temperature and pressure (STP)] of the gas desorbed from film, A is the film surface area of both lateral sides, L is the film thickness, and D is the diffusivity of the gas. Figure 2 contains a schematic explanation for the evaluation of D from a graphical analysis of the D-curve simulated at the gas sorption amount of 1.0 cm^3(STP)/cm^3 ($=C_A$). Figure 3 shows dN_A/dt as a function of the residual amount of sorbed gas in film ΔC_A. The plots obtained give a good straight line, and the diffusivity was calculated as $D = 5.0 \times 10^{-8}$ cm^2/s from a slope of the straight line by using Eq. (1).

For the application of the FPD method, the following assumptions should be satisfied: (1) The molecular structure of the polymeric film is identical before and after the FPD operation; (2) The sorbed gas is uniformly distributed in the film; (3) The rate of gas

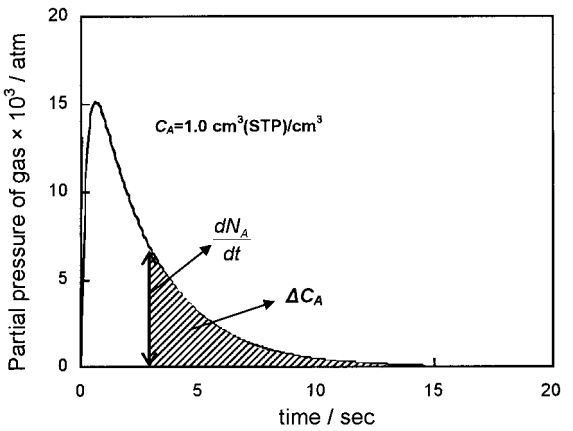

Figure 2 Schematic explanation for the evaluation of gas diffusivity from D-curve.

desorption from the film equals the gas diffusion rate in the film; (4) The diffusion rate from the surface to the center of a film section equals that from the center to the surface; (5) The gas diffusion rate evaluated from the D-curve equals the rate evaluated from the conventional gas permeation experiment; (6) The helium gas used as a carrier gas does not influence the D-curve. The validity of assumption (1) is reconfirmed by evidence that the D-curves were not influenced by the repeated FPD operation using the same film. Assumption (2) is reasonably accepted because of the sufficiently thin films used in this study. In this case, one can use analogies with adsorbed gas species forming a monolayer on a solid surface: the desorption rate of the adsorbed species is proportional to the amount of sorbed gas, and the total adsorbed amount becomes a driving force of the desorption rate. For assumption (3), in thin film, the desorption of gas from the film is a rate determining step in an overall mass transfer process, which means the desorption rate is equal to the diffusion rate. For assumptions (4) and (5), the D-curve is obtained under an unsteady state unlike the steady-state conditions in conventional methods. The assumption means a reversible mass-transfer process of gas in a film matrix between the unsteady state and the steady state without depending on the gas diffusion direction from the center to the surface or from the surface to the center of the film. This assumption is acceptable for a homogeneously prepared thin film. For assumption (6), it was reconfirmed that the evaluated diffusivity of CO_2 always gave the same value without depending on the size of the D-curves, which were obtained by changing the concentration of CO_2 in helium. This result means that the diffusivity of CO_2 is not influenced by the adsorbed amount of He.

For the graphical analysis of the D-curves obtained in the FPD method, a gas desorption model was proposed. At the D-period, under the assumption of complete mixing in the sorption cell, a material balance equation for the desorption of gas component A can be derived as

$$\frac{V - V_M}{RT}\frac{dp_A}{dt} = \frac{2AD}{L}\Delta C_A - v_0\frac{p_A}{RT} \tag{2}$$

where p_A is the partial pressure of gas component A in the cell, which is equal to one at the outlet of the sorption cell; v_0 is the flow rate of the carrier gas (He) measured at the outlet of the gas-sorption cell; V_M is the apparent membrane volume; V is the cell volume; ϵ is the void fraction of the sample cell [$\epsilon = (V - V_M)/V$]; R is the gas constant; and T is the temperature at the outlet of the gas-sorption cell.

Assuming the change in carrier gas-flow rate caused by the gas desorption from film to be negligibly small and taking into account the initial conditions of $p_A = 0$ and $\Delta C_A = C_A$ (C_A is the equilibrium amount of sorbed gas in film) at $t = 0$, Eq. (1) is solved as

$$\Delta C_A = C_A e^{-\gamma t} \tag{3}$$

where

$$\gamma = \frac{2DA}{V_M L}$$

Equation (3) is inserted into Eq. (2), and Eq. (2) is rewritten as

$$\frac{dp_A}{dt} + ap_A = \beta C_A e^{-\gamma t} \tag{4}$$

where

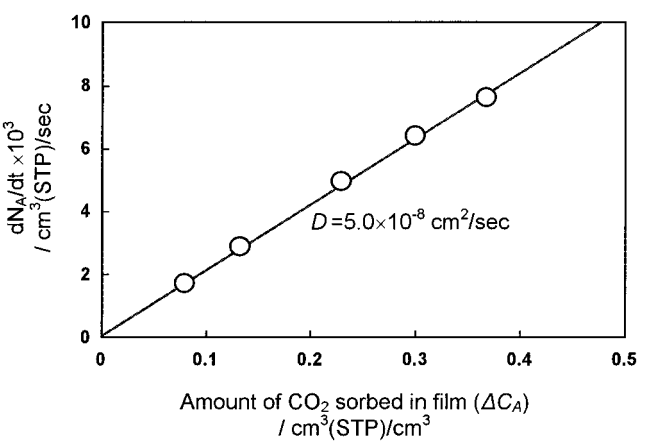

Figure 3 The desorption rate of sorbed gas as a function of ΔC_A.

TABLE I
Characteristics of the Polymeric Films Used

	Density (g/cm^3)	Thickness (μm)
LDPE	0.927	49
PC	1.2	50
PS	1.1	30

$$\alpha = \frac{v_0}{\epsilon V}, \quad \beta = \frac{2DA}{L}\frac{RT}{\epsilon V}$$

The solution to Eq. (4) is given as

$$p_A = \frac{\beta\, C_A}{\alpha - \gamma}(e^{-\gamma t} - e^{-\alpha t}) \tag{5}$$

EXPERIMENTAL

Materials and procedure

Table I shows characteristics of three polymeric films used in this study: LDPE used as a reference film for rubbery polymeric films, polystyrene (PS), and polycarbonate (PC) for glassy polymeric films. All sample films used in this study were supplied from Tama-Poly Inc., Tokyo, Japan. Carbon dioxide (CO_2, 99.5%) for a sorption gas and helium (He, 99.99%) for a carrier gas of the experimental system were used without further purification. All gases were obtained from Air Water Inc., Sapporo, Japan.

Figure 4 contains a schematic drawing of the experimental setup used in this study. About 3.0 g of film samples (30–50 μm in thickness) was put into a gas-sorption cell (40 cm^3) made of Pyrex glass or stainless steel, and the cell was placed in a water bath that was carefully controlled at 25 ($\pm$0.1)°C for 24 h up to the completion of CO_2 gas sorption equilibrium. The temperature in the cell was always monitored by using a CA thermocouple. The typical transient response curves of the temperature characterized by the three operations (F-, P-, and D-operations) are, respectively, shown by curves (b), (c), and (d) in Figure 1. After the CO_2 sorption equilibrium was completed, in the F-period, the cell was moved from the water bath to a liquid nitrogen bath (−196°C) for the fixation of sorbed CO_2 in the film. The CO_2 gas stream was switched over to a helium gas stream of 75 cm^3/min when the cell temperature was decreased to less than −78°C. After the film sample was exposed to the He stream at −196°C for 5 min, in the P-period, the liquid nitrogen bath was replaced by an ethanol bath of −78°C. By this stepwise increase of temperature accompanied by the He–gas stream treatments for 1 h, the residual CO_2 gas and physically adsorbed CO_2 in the cell were sufficiently removed. At the D-period, the ethanol bath was then replaced by an ice–salt bath, which was previously kept at −9($\pm$2.0)°C, and the response of CO_2 desorbed from the film was followed as continuously as possible by using a gas chromatograph (GC) attached with a six-way valve with a gas sample tube of about 1 cm^3. In this procedure, −9°C was chosen because the desorption rate of CO_2 at 25°C was too fast to follow the D-curve by the GC.

For the transient response of temperature, the time delays caused by the experimental apparatus used were evaluated within 2 to 3 min for the F- and P-periods and at about 2.5 min for the D-period up to 90% of the objective temperature. CO_2 was analyzed by gas chromatography (TCD, Shimadzu GC-8A) under the following conditions: column, 100 × 0.3 cm OD stainless steal packed with Porapack-Q; temperature: injector, 80°C; column and detector, 60°C. At all time intervals, a 1-mL sample of desorbed gas from the outlet of the gas sorption cell was injected by a six-way valve equipped with a sampling tube.

To evaluate the time delay of the gas-chromatographic analysis technique used in this study, a continuous evaluation technique using a thermal conductivity detector and CO_2 gas was applied, and the mode of the conductivity response curves of CO_2 obtained was almost the same as the mode of the GC technique indicated.

Blank test and error evaluation

To determine the validity of the transient response of gas in the sample cell (40 cm^3), special attention should be given to the response curve of CO_2. For the blank test to evaluate an error derived from the physical adsorption component of CO_2 that could appear on an apparent surface of membrane and an inner wall of the cell, nonporous glass beads were packed into the cell instead of sample films. The beads (60 g) were about 1 mm in diameter and 1200 cm^2 of the total surface area, which was the same as the one used for the sample film. The blank transient responses of tem-

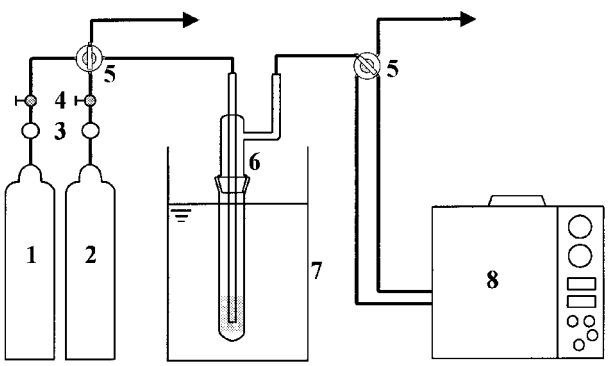

1. He gas cylinder
2. CO_2 gas cylinder
3. Stop valve
4. Mass flow meter
5. Four way valve
6. Pyrex glass tube for gas sorption
7. Water bath (or liquid nitrogen and ethanol bath)
8. Gas chromatography (TCD)

Figure 4 Schematic drawing of the experimental setup used in this study.

perature and CO_2 were carefully conducted by using the same conditions as the sample film-packed cell, and the two response curves obtained were, respectively, compared to the response curves of temperature and CO_2 gas monitored for the sample films as shown by [(a–d)] and CO_2 gas [(a′–d′)] curves in Figure 1. The temperature-response curves clearly show good agreement between the blank cell (broken line) and the sample cell [solid line; curves (b), (c), and (d)]. The blank response curve of CO_2 (closed circle), on the other hand, proved no desorption of CO_2 at the D-period [closed circle, curve (d′)], even though it indicates good agreement with the sample curves (open circle) in the F- and P-periods [curves (a′–c′)]. From these results, one can reconfirm that the D-curve of CO_2 (open circle) obtained at the D-period was caused by the actual desorption of CO_2 sorbed in the film.

The system errors derived from the experimental operation were carefully evaluated based on the deviations in operating parameters from the objected values. In the experimental measurements, special attention should be paid to the D-period operation. The results propose possible errors of less than 7% at most for the constancy of the He-stream flow rate, cell-temperature constancy, minimization of gas bypassing the cell, and gas analysis by using the gas chromatograph.

The limitation of the FPD method to apply polymeric films is considered to be because of the working limitations of analytical equipment and experimental devices as the time period of the D-curve is more than a few minutes when gas chromatography is used and the appropriate dimensions of sample tube and membrane samples are prepared.

RESULTS AND DISCUSSION

Interpretation of desorption response curves

Figure 5 illustrates the D-curves of CO_2 for the LDPE, PC, and PS films at −9°C. The graphical integration of the three response curves obtained evaluates the amount of CO_2 sorbed in the films (C_{CO2}) at 25°C as 0.31 cm^3(STP)/cm^3 for LDPE, 6.7 cm^3(STP)/cm^3 for PC, and 3.9 cm^3(STP)/cm^3 for PS. C_{CO2}'s for the PC and PS films are one order larger than that of the LDPE film.

Based on the procedure presented in Figure 3, the desorption rate of CO_2 can easily be evaluated. Figure 6 illustrates the desorption rate of CO_2 (dN_{CO2}/dt) for the LDPE, PC, and PS films as a function of the amount of CO_2 sorption (ΔC_{CO2}). The LDPE film gives a single straight line, whereas the PS and PC films clearly exhibit a characteristic straight line with an inflection point. This difference in the straight lines is caused by the polymeric structure difference between

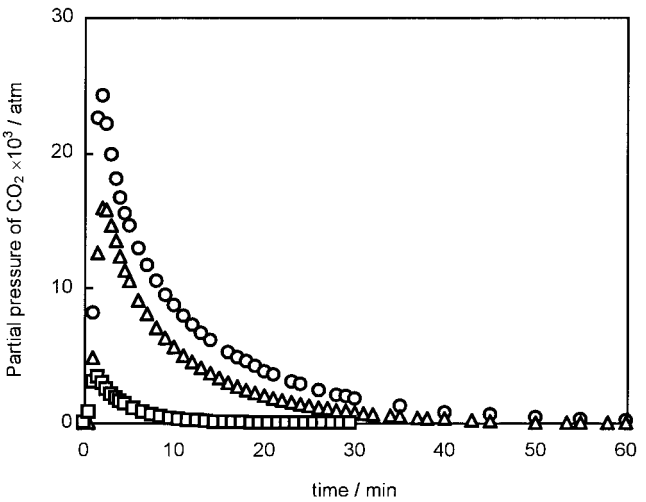

Figure 5 Desorption response curves of CO_2 for LDPE, PC, and PS at −9°C. ○: PC; △: PS; □: LDPE.

rubbery and glassy polymers, clearly visualizing the difference in the gas diffusion mechanism. For the PC and PS films as glassy polymers, one may recognize two regions divided at the inflection point, Regions I and II, as shown in Figure 6.

Quantitative discrimination of the Henry and the Langmuir modes

As was reported by Paul and Koros,[4] it is generally understood that Henry mode diffusivity (D_D) is about one order higher than Langmuir mode diffusivity (D_H) calculated from the partial immobilization model, and the two modes simultaneously and individually progress. Based on these considerations, one can reasonably attribute Region I in Figure 6 to a Langmuir mode desorption process and Region II to a complex period of the desorption processes of both the Henry and the Langmuir modes. To explain this characteristic mode, based on the parallel diffusion of the Henry and Langmuir modes, one can propose a dual-desorption model which is described by Eq. (6):

$$p_A = p_D + p_H \tag{6}$$

$$p_D = \frac{\beta_D C_D}{\alpha - \gamma_D}\left(e^{-\gamma_D t} - e^{-\alpha t}\right) \tag{7}$$

$$p_H = \frac{\beta_H C_H}{\alpha - \gamma_H}\left(e^{-\gamma_H t} - e^{-\alpha t}\right) \tag{8}$$

$$\alpha = \frac{v_0}{\epsilon V}, \quad \beta_D = \frac{2D_D A}{L}\frac{RT}{\epsilon V}, \quad \beta_H = \frac{2D_H A}{L}\frac{RT}{\epsilon V},$$

$$\gamma_D = \frac{2D_D A}{V_M L}, \quad \gamma_H = \frac{2D_H A}{V_M L}$$

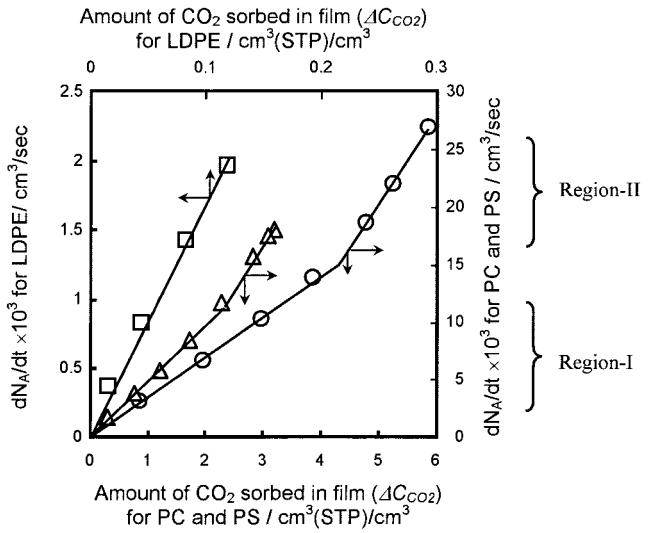

Figure 6 Desorption rates of CO_2 at −9°C for LDPE, PC, and PS films as a function of ΔC_{CO2}.

where D_D, D_H and C_D, C_H are diffusivity (cm^2/s) and sorbed amounts [cm^3(STP)/cm^3] for the Henry (subscript D) and Langmuir (subscript H) modes, respectively.

Consequently, D_H can be evaluated from the slope of the straight line in Region I as $D_H = 8.06 \times 10^{-9}$ (−9°C) for PS and $D_H = 3.06 \times 10^{-9}$ (−9°C) cm^2/s for PC. The value of C_H was then calculated from Eq. (8) by using the D_H values evaluated to be 2.79 and 5.87 cm^3(STP)/cm^3 for PS and PC, respectively. By using

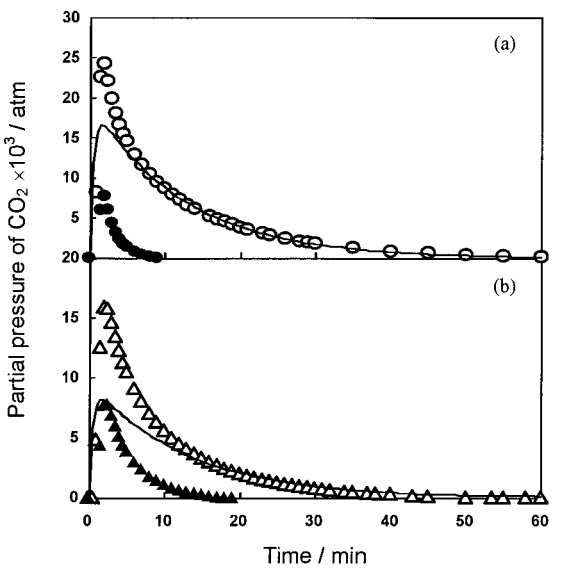

Figure 7 Discrimination of the desorption response curves of CO_2 for the PC (a) and PS (b) films at the D-period and −9°C, based on the dual desorption model. ○: PC; △: PS. Open and closed symbols are experimental and Henry mode curves, respectively. The solid lines are calculated curves based on the Langmuir mode.

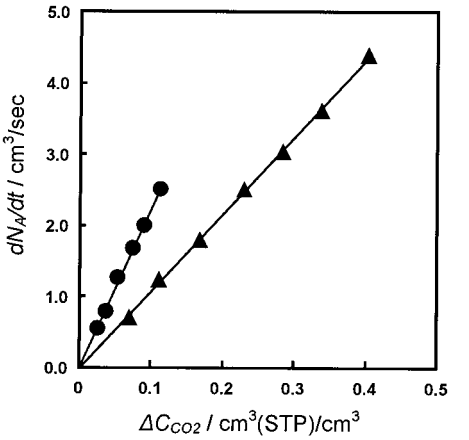

Figure 8 Linear plots of the Henry mode rates as a function of ΔC_{CO2} for PC (●) and PS (△) at −9°C. The slopes of the lines propose D_D.

the D_H and C_H values obtained thus, the Langmuir mode desorption curves can be simulated by using Eq. (8) as shown by the solid-line curves in Figure 7(a, b). From the assumption of the dual-permeation model described above, because the desorption curve of glassy polymeric film consists of the curve of the Henry mode plus the Langmuir mode, the curve of the Henry mode can easily be drawn by an arithmetical calculation as the experimental curve minus the Langmuir mode curve. The results obtained for the PC and PS films are presented by the closed circle (a) and closed triangle (b), respectively, in Figure 7. The Henry mode curves obtained thus for PC (a) and PS (b) films are graphically analyzed to evaluate D_D and C_D by using the procedure used for Figures 2 and 3. Figure 8 illustrates dN_{CO2}/dt as a function of ΔC_{CO2} for the Henry mode desorption. D_D values calculated from the slope of straight line are 20.2×10^{-9} cm^2/s for PC and 24.8×10^{-9} cm^2/s for PS. From the graphical integration of the two curves (closed circle and closed triangle) in Figure 7, C_D and C_H values are evaluated as 1.05 and 2.79 cm^3(STP)/cm^3 for PS and 0.58 and 5.87 cm^3(STP)/cm^3 for PC, respectively. All of the four parameters obtained are summarized in Table II. The sorption amount of Langmuir mode is 2.6–10 times larger than that of the Henry mode, and the diffusivity of the Henry mode (D_D) is about 3–6.6 times larger than that of the Langmuir mode (D_H). The value of D_H/D_D is 32.5–15.1%, which is larger than the 10% proposed in Koros and Paul's works.[10] The reason for this discrepancy is difficult to understand from the present work because of the indirect examination of the two values. To draw exact conclusions, further detailed experimental work is needed.

In proving the validity of the four parameters obtained by the FPD method, the values should be directly compared to the values obtained from the conventional techniques. Unfortunately, we have no data

TABLE II
The Parameters Calculated from the Dual Desorption Model

Film	C_D [cm^3 (STP)/cm^3]	C_H [cm^3 (STP)/cm^3]	$D_D \times 10^9$ (cm^2/s)	$D_H \times 10^9$ (cm^2/s)
PS	1.05 (25°C)	2.79 (25°C)	24.8 (−9°C)	8.06 (−9°C)
PC	0.58 (25°C)	5.87 (25°C)	20.2 (−9°C)	3.06 (−9°C)

on the conventional techniques obtained for the same experimental conditions. For a rough comparison, even though the temperatures differ, one can use several values evaluated by the conventional methods appearing in the literature. The reference data obtained at 35°C are summarized in Table III, where C_D and C_H were calculated by the dual-sorption model by using the data obtained from the pressure-decay method[6–8,13,14] and D_D and D_H were evaluated by linearization analysis based on the partial-immobilization model.[13] The rough linear relation between the reference and the FPD method strongly suggests a similar tendency of the four parameter values to be meaningful from the physicochemical point of view (general understanding of $C_D < C_H$ and $D_D > D_H$), although the different permeation temperatures differ.

Parameter sensitivity against the D-curve mode

Focusing on how the mode of the D-period response curve is sensitively influenced by a change in the values of C_D, C_H, D_D, and D_H, one can evaluate the availability of the discrimination technique by using the FPD method. Figure 9 illustrates a characteristic change in the mode of two D-curves for the PC film visualized by a computer simulation technique by using the following two parameter groups: (1) C_D = 0.58, C_H = 5.87 cm^3(STP)/cm^3, D_D = 20.2, and D_H = 3.06 $\times$ 10^{-9} cm^2/s evaluated from the FPD method (FPD-curve) and (2) C_D = 0.99, C_H = 5.45 cm^3(STP)/cm^3, D_D = 46.7, and D_H = 4.72 $\times$ 10^{-9} cm^2/s calculated from the Koros procedure[13] (Koros curve). Comparing the two D-curves at the initial stage, the peak height of the Koros curve is 1.8 times higher than that of the FPD-curve because the D_D value (Koros) is 2.3 times higher than the D_D (FPD), whereas, at the later period of time when the D-curve reaches zero, the Koros curve takes 35 min, 50 min less than the FPD curve, because the D_H value (Koros) is 1.5 times larger than the D_H (FPD). From these results, one can recognize that the graphical analysis of the D-curve from the FPD method sensitively discriminates the variety of D_D and D_H values characterized by the diffusion of the Henry and Langmuir modes.

CONCLUSION

The FPD method proposed quantitatively discriminated the four gas permeation parameters (C_D, C_H, D_D, and D_H) for glassy polymeric film by using CO_2 gas and PS and PC films. The mode of the CO_2 gas desorption response curve (D-curve) obtained was sensitively characterized by the variety of the four parameters. To describe the D-curves of CO_2 for the PS and PC films, the dual-desorption model was proposed, and a mathematical model was derived to consistently interpret the experimental D-curves obtained. The conclusions obtained are as follows:

(1) The graphical analysis of the D-curve exactly demonstrated the complex mode of the Henry mode and Langmuir mode desorptions, advantageously characterized at the initial stage, and the Langmuir mode desorption at the later stage of the D-curve.

(2) The inflection point of the straight line for the desorption rate as a function of the residual sorption amount could be effectively used to distinguish the gas diffusion mechanism shift from the Langmuir–Henry complex mode to the Langmuir mode.

TABLE III
Parameters Calculated from the Dual Sorption and the Partial Immobilization Models

Film	C_D [cm^3 (STP)/cm^3]	C_H [cm^3 (STP)/cm^3]	$D_D \times 10^9$ (cm^2/s)	$D_H \times 10^9$ (cm^2/s)	Authors
PS (oriented)	0.57	2.42	—	—	W. R. Veith[6]
PS (unoriented)	0.65	2.85	—	—	
PS	0.80	1.74	—	—	E. Sada[14]
PS	0.54	1.67	—	—	P. C. Raymond[7]
PC	0.99	5.45	46.7	4.72	W. J. Koros[13]
PC	0.77	14.3	—	—	W. R. Vieth[8]
PC	0.91	6.09	—	—	E. Sada[14]

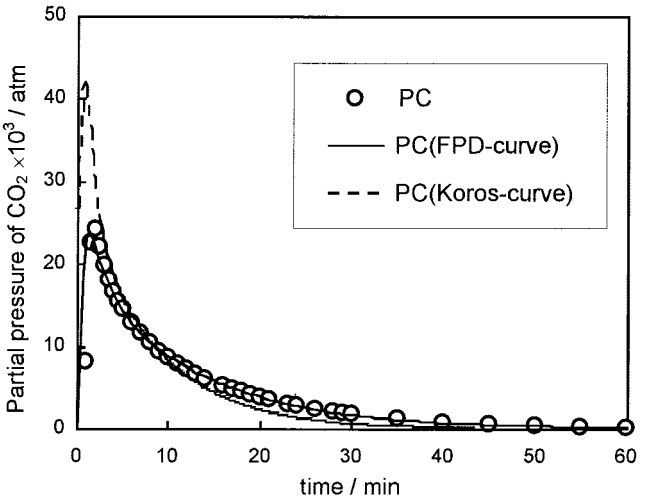

Figure 9 Comparison of simulated curves evaluated by the experimental and reference values.

(3) The obtained values of the four parameters (C_D, C_H, D_D, and D_H) fall on a conventional meaningful straight line, indicating $C_H > C_D$ and $D_D > D_H$.

Nomenclature

A	film surface area [cm^2]
C_A	equilibrium amount of gas sorbed in film [cm^3(STP)/cm^3]
ΔC_A	residual amount of gas sorbed in film [cm^3(STP)/cm^3]
ΔC_{CO2}	residual amount of CO_2 sorbed in film [cm^3(STP)/cm^3]
C_D	concentration of Henry dissolution component [cm^3(STP)/cm^3]
C_H	concentration of Langmuir adsorption component [cm^3(STP)/cm^3]
D	diffusivity [cm^2/s]
D_D	diffusivity of Henry mode [cm^2/s]
D_H	diffusivity of Langmuir mode [cm^2/s]
dN_A/dt	desorption rate of gas component A [cm^3(STP)/s]
dN_{CO2}/dt	desorption rate of CO_2 [cm^3(STP)/s]
L	film thickness [cm]
p_A	partial pressure of gas component A [atm]
R	gas constant [cm^3 atm/mol K]
S	solubility [cm^3(STP)/cm^3 cmHg]
T	temperature at the outlet of gas sorption cell [K]
t	desorbed time [s]
V	volume of gas sorption cell [cm^3]
V_M	volume of film [cm^3]
v_0	flow rate of carrier helium gas [cm^3/s]

References

1. Crank, J.; Park, G. S. Diffusion in Polymers; Academic Press: New York, 1968.
2. Felder, R. M.; Huvard, G. S. Meth Exp Phys 1980, 16C, 315.
3. Barrer, R. M.; Barrie, J. A.; Slater, J. J Polym Sci 1958, 27, 177.
4. Paul, D. R.; Koros, W. J. J Polym Sci 1976, 14, 675.
5. Vieth, W. R.; Frangoulis, C. S.; Rionda, J. A. J Colloid Interface Sci 1966, 22, 454.
6. Vieth, W. R.; Tam, P. M.; Michaels, A. S. J Colloid Interface Sci 1966, 22, 360.
7. Raymond, P. C.; Paul, D. R. J Polym Sci, Part B: Polym Phys 1990, 28 2079.
8. Vieth, W. R.; Elinberg, J. A. J Appl Polym Sci 1972, 16, 945.
9. Toi, K.; Maeda, Y.; Tokuda, T. J Membr Sci 1983, 13, 15.
10. Koros, W. J.; Paul, D. R. J Polym Sci, Polym Phys Ed 1978, 16 1947.
11. Stern, S. A.; De Meringo, A. H. J Polym Sci, Polym Phys Ed 1978, 16, 735.
12. Stern, S. A.; Kulkarni, S. S. J Membr Sci 1982, 10, 235.
13. Koros. W. J.; Paul, D. R.; Rocha, A. A. J Polym Sci, Polym Phys Ed 1976, 14, 687.
14. Sada, E.; Kumazawa, H.; Yakushiji, H.; Bamba, Y.; Sakata, K.; Wang, S.-T. Ind Eng Chem Res 1987, 26, 433.
15. Kumazawa, H.; Wang, J.-S.; Fukuda, T.; Sada, E. J Membr Sci 1994, 93, 53.
16. Wang, R.; Chan, S. S.; Liu, Y.; Cung, T. S. J Membr Sci 2002, 199, 191.
17. Togawa, J.; Horiuchi, J.; Kanno, T.; Kobayashi, M. J Membrane Sci 2001, 182, 125.
18. Togawa, J.; Kanno, T.; Horiuchi, J.; Kobayashi, M. Proc Eng Membr 2001, 2, 417.